

Entanglement in Cascaded-Crystal Parametric Down-Conversion

Mete Atatüre, Alexander V. Sergienko, Bahaa E. A. Saleh, and Malvin C. Teich

*Quantum Imaging Laboratory, Departments of Electrical & Computer Engineering and Physics,
Boston University, 8 Saint Mary's Street, Boston, Massachusetts 02215*

(Received 21 December 2000)

We use spontaneous parametric down-conversion in a cascade of crystals, driven by a single monochromatic cw pump laser, to study the interference of entangled photon pairs. By changing the distance between the crystals, the observed quantum interference pattern varies continuously from that associated with a longer single crystal to that associated with independent emissions from two distinct crystals. Postselection via spectral filtering suppresses this phenomenon. These findings are expected to advance the field of quantum-state engineering.

DOI: 10.1103/PhysRevLett.86.4013

PACS numbers: 42.50.Dv, 03.65.Ta, 42.65.Ky

A good deal of research has been carried out in recent years with the help of entangled-photon states. A standard source of such nonclassical light comprises a highly coherent pump laser incident on a nonlinear optical crystal; beams of entangled-photon pairs (twin-photon beams) are generated via spontaneous optical parametric down-conversion (SPDC) [1]. Depending on the configuration of the experiment and the cut of the crystal, the photon pairs can be entangled in any number of variables: time, frequency, direction of propagation, and polarization. Studies carried out with twin-photon beams range from the examination of quantum paradoxes [2–4], to applications in optical measurements [5], spectroscopy [6], imaging [7], and quantum information [8,9].

Quite recently, because of practical advances in the engineering of special quantum states [10,11], studies of the coherence properties of entangled states generated via parametric down-conversion have taken center stage. Since entanglement from multiple sources is of fundamental importance in quantum mechanics it is crucial to examine its nature in the simplest of circumstances, viz. in the absence of possible confounding effects such as those associated with predetector spectral and spatial filtering. To this end we have carried out a study of the fourth-order coherence properties of entangled-photon states generated in a medium comprising two separate nonlinear crystals pumped by the same highly coherent, monochromatic continuous wave (cw) laser source. We show that, depending on the spacing between the crystals, the observed quantum interference pattern can be varied from that associated with a longer single crystal to one associated with independent emissions from two distinct crystals.

The results reported in this Letter are likely to be of use in guiding future developments in the area of complex quantum-state engineering involving multicrystal configurations [12], in ultrafast-pumped parametric down-conversion [11], and in the design of periodically poled materials for nonlinear-optics applications [13].

Quantum-interference experiments with a two-crystal cascade.—The experimental arrangement is illustrated in Fig. 1. A 100-mW cw Ar⁺-ion laser operated at 351.1 nm

served as the pump. This highly monochromatic, coherent ultraviolet light was passed sequentially through a cascaded pair of beta-barium-borate (BBO) crystals of lengths 1.5 and 0.5 mm. The distance between the crystals was nominally 5.5 cm. The crystals served as nonlinear optical media in which orthogonally polarized (type-II) spontaneous parametric down-conversion was generated in a collinear degenerate configuration ($\omega_s^0 = \omega_i^0 = \omega_p^0/2$, where ω_s^0 , ω_i^0 , and ω_p^0 represent the central frequencies of the signal, idler, and pump fields, respectively). The laser power was sufficiently low to provide, with high probability, that at most one photon pair was generated at a given time (the high visibilities obtained from separate single-crystal quantum-interference experiments confirm the validity of this assumption).

Collinear down-converted beams were selected by a 2.0-mm circular aperture (not shown), located 1 m beyond the second crystal. After removal of the residual pump-laser beam by a fused-silica dispersion prism, the

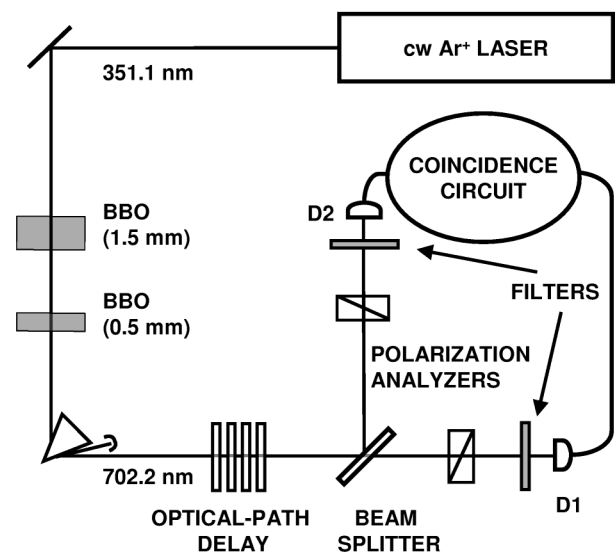


FIG. 1. Schematic diagram of the cw cascaded-crystal quantum-interference experiment.

twin-photon beams were passed through a birefringent crystalline-quartz element of variable thickness, which served to introduce optical-path delay. The entangled-photon beams were then directed to a nonpolarizing beam splitter, and thence to the two arms of a polarization intensity interferometer. Each arm of the interferometer comprised a Glan-Thompson polarization analyzer set at 45° with respect to the horizontal axis in the laboratory frame, which established the basis for the polarization measurements. Finally a convex lens (not shown) was used to reduce the beam size to that of the small area of the actively quenched Peltier-cooled avalanche-photodiode detector. Predetection spectral filters were used in some experiments. A coincidence circuit with a 3-nsec integration window constituted the basic electronics of the experiment. Corrections for accidental coincidences were not necessary. In each of the interference experiments, the coincidence counts were accumulated over a period of 30 sec and plotted against the optical-path delay τ in fsec.

When no filters were used we find that, as the separation between the crystals is varied, the coincidence pattern changes in nature between the two extremes shown in Fig. 2 (filled and open squares). This change occurs over a distance of a few mm of crystal separation; changes over scales of the order of the optical wavelength have no noticeable effect. We will demonstrate elsewhere that this is attributable to angular spread in the down-converted beams. The solid curves represent the theoretical results based on a model introduced in the next section, which are fit to data taken at the two extremes. The results of a similar experiment, in which 9-nm-bandwidth (FWHM) filters

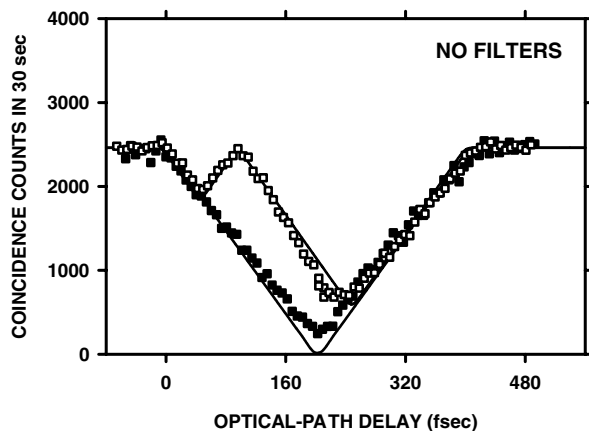


FIG. 2. Coincidence counts, $R(\theta_1 = 45^\circ, \theta_2 = 45^\circ, \tau)$, as a function of relative optical-path delay, τ , for the relative phase settings $\phi_1 - \phi_2 = 0$ (solid squares) and $\phi_1 - \phi_2 = \pi/2$ (open squares), in the absence of predetection filtering. The solid curves are the theoretical plots corresponding to Eqs. (7) and (8). The fourth-order interference pattern which results when the phases ϕ_1 and ϕ_2 differ by $\pi/2$ explicitly reveals the order in which the crystals are cascaded; the second (thin) crystal provides a background coincidence rate for the first (thick) crystal. The fourth-order interference pattern when the phases ϕ_1 and ϕ_2 differ by 0 forms a single triangular dip, just as if a single nonlinear crystal were used.

were placed immediately before each of the detectors, are shown in Fig. 3. The solid curves again represent the theoretical results.

Theory.—We proceed to provide a phenomenological model that is consistent with all of our experimental observations. We represent the overall quantum state as arising from a general superposition of two Hamiltonians that govern the parametric down-conversion generated from each crystal with the appropriate phases. The two-photon state $|\Psi^{(2)}\rangle$ at the output of a cascade of two crystals can be written as the sum

$$|\Psi^{(2)}\rangle \sim |0\rangle - \frac{i}{\hbar} \int dt [e^{i\phi_1} \hat{H}_{\text{int}}(t, L_1) + e^{i\phi_2} \hat{H}_{\text{int}}(t, L_2)] |0\rangle, \quad (1)$$

where $|0\rangle$ denotes the unperturbed initial vacuum state; L_1 and L_2 represent the lengths of the two down-conversion crystals; and ϕ_1 and ϕ_2 are phases associated with the down-converted waves generated by the two crystals. For one-dimensional (along the z -axis) collinear degenerate type-II SPDC from a single crystal of length L , the Hamiltonian in Eq. (1) is described by [1]:

$$\hat{H}_{\text{int}}(t, L) \sim \chi^{(2)} \int_{-L}^0 dz E_p(t, z) \hat{E}_s^{(-)}(t, z) \hat{E}_i^{(-)}(t, z) + \text{H.c.} \quad (2)$$

Here $\chi^{(2)}$ is the second-order nonlinear susceptibility of the medium; $E_p(t, z)$ is the electric field of the classical pump at the time t , $\hat{E}_s^{(-)}(t, z)$ and $\hat{E}_i^{(+)}(t, z)$ represent the negative- and positive-frequency portions of the down-converted-beam electric-field operators, respectively; and

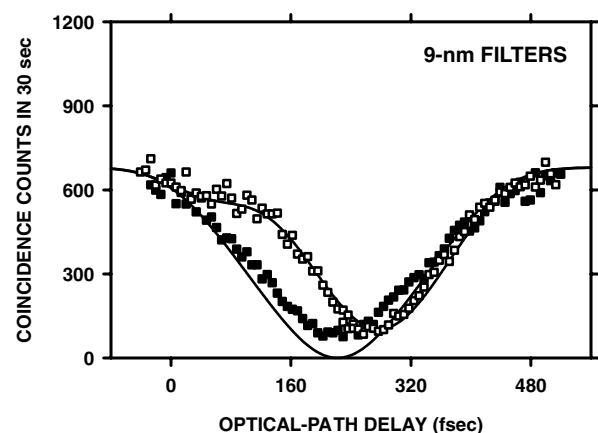


FIG. 3. The same as Fig. 2, but now in the presence of 9-nm-bandwidth filters placed immediately before detectors D1 and D2 (Fig. 1). The spectral postselection provided by the filtering transforms the interference pattern into a function with a single dip that partially masks the crystal configuration. In experiments using yet narrower bandwidth filters (not shown), the coincidence rate is predicted and observed to be indistinguishable from that obtained using down-conversion from a single crystal, giving the illusion that the dual-crystal and single-crystal down-conversion quantum states are identical for all values of $\phi_1 - \phi_2$.

H.c. stands for Hermitian conjugate. The subscripts p, s, i represent the pump, signal, and idler, respectively. It is clear that $|\Psi^{(2)}\rangle$ in Eq. (1) is equivalent to that produced by a longer single crystal when $\phi_1 - \phi_2 = 0$.

The coincidence-detection probability amplitude is calculated from [14]

$$\mathcal{A}(t_1, t_2) = \langle 0 | \hat{E}_1^{(+)} \hat{E}_2^{(+)} | \Psi^{(2)} \rangle, \quad (3)$$

where t_1 and t_2 denote the photon arrival times at detectors D1 and D2, respectively.

For the experimental configuration shown in Fig. 1, in the general case where predetection filters may be present, the probability amplitude given by Eq. (3) takes the form

$$\begin{aligned} A(T, t) &\equiv \mathcal{A}(t_1, t_2) \\ &\sim \sqrt{I_p} e^{-i\omega_p T} [e^{i\phi_1} \mathcal{F}_1(t - DL_2, \sigma_f) \\ &\quad + e^{i\phi_2} \mathcal{F}_2(t, \sigma_f)], \end{aligned} \quad (4)$$

$$\begin{aligned} R(\theta_1, \theta_2, \tau) &= I_p \int_{-\infty}^{\infty} \int_{-\infty}^{\infty} dT dt |e^{i\phi_2} [\cos\theta_1 \sin\theta_2 \mathcal{F}_2(t + \tau, \sigma_f) - \sin\theta_1 \cos\theta_2 \mathcal{F}_2(-t + \tau, \sigma_f)] \\ &\quad + e^{i\phi_1} [\cos\theta_1 \sin\theta_2 \mathcal{F}_1(t + \tau - DL_2, \sigma_f) - \sin\theta_1 \cos\theta_2 \mathcal{F}_1(-t + \tau - DL_2, \sigma_f)]|^2. \end{aligned} \quad (6)$$

We have found that our experimental observations at an arbitrary separation between the crystals can be described in terms of $\phi_1 - \phi_2$. In the limit $\phi_1 - \phi_2 = 0$, the coincidence rate in Eq. (6) reduces to

$$R(\theta_1, \theta_2, \tau) = I_p \int_{-\infty}^{\infty} \int_{-\infty}^{\infty} dT dt |\cos\theta_1 \sin\theta_2 \mathcal{F}_{1+2}(t + \tau, \sigma_f) - \sin\theta_1 \cos\theta_2 \mathcal{F}_{1+2}(-t + \tau, \sigma_f)|^2, \quad (7)$$

where the function \mathcal{F}_{1+2} is associated with a single nonlinear crystal of length $L = L_1 + L_2$. The resultant quantum-interference pattern then assumes the classic form of a single dip with a width determined by L .

In the limit $\phi_1 - \phi_2 = \pi/2$, on the other hand, Eq. (6) becomes

$$R(\theta_1, \theta_2, \tau) = R_1(\theta_1, \theta_2, \tau - DL_2) + R_2(\theta_1, \theta_2, \tau), \quad (8)$$

with $R_1(\theta_1, \theta_2, \tau - DL_2)$ and $R_2(\theta_1, \theta_2, \tau)$ representing the coincidence rates arising from down-conversion generated independently at the two crystals. In this case the quantum-interference pattern assumes the form of two adjacent dips. This is the same result that would be obtained if the phases ϕ_1 and ϕ_2 in Eq. (1) were taken to be statistically independent and uniformly distributed over the range $[0, 2\pi)$. Finally, in the general case of an N -crystal cascade in this same limit, the overall coincidence rate becomes

$$R(\theta_1, \theta_2, N, \tau) = \sum_{i=1}^N R_i \left(\theta_1, \theta_2, \tau - \sum_{j=i+1}^N DL_j \right), \quad (9)$$

where the summation over j accounts for dispersion delays introduced by all crystals subsequent to the i th.

The coincidence rate predicted by Eqs. (7) and (8), for $\phi_1 - \phi_2 = 0$ and $\phi_1 - \phi_2 = \pi/2$, respectively, are plotted in Fig. 2. For BBO material of overall length $L = L_1 + L_2 = 2$ mm, $\theta_1 = \theta_2 = 45^\circ$, and in the absence of predetection filtering, Eq. (7) is plotted as the single-

where $T = (t_1 + t_2)/2$, $t = (t_1 - t_2)$, and $D = (\frac{1}{v_i} - \frac{1}{v_s})$ with v_i and v_s representing the group velocities of the idler and signal waves, respectively. I_p is the mean pump intensity. For Gaussian-shaped filters, the function \mathcal{F}_i , $i = 1, 2$, depends on the $1/e$ -spectral-filter bandwidth σ_f via

$$\mathcal{F}_i(t, \sigma_f) = \frac{1}{2DL_i} \left\{ \operatorname{erf} \left(\frac{\sigma_f}{2} t \right) - \operatorname{erf} \left[\frac{\sigma_f}{2} (t - DL_i) \right] \right\}. \quad (5)$$

In the absence of filtering, $\mathcal{F}_i(t, \sigma_f)$ becomes a rectangular function that assumes unity value in the range $[-DL_i, 0]$, and zero elsewhere, as expected.

Using Eq. (4), the coincidence rate $R(\tau)$ can be explicitly written in terms of polarization-analyzer angles (θ_1, θ_2) defined with respect to the laboratory coordinate system's horizontal axis (which is set at zero degrees) [14]:

dip solid curve in Fig. 2, which agrees well with the associated experimental data (filled squares). The coincidence rate provided in Eq. (8), in contrast, applies when ϕ_1 and ϕ_2 are out of phase with each other by $\pi/2$. Using the same experimental parameters, this function is plotted as the double-dip solid curve in Fig. 2, which also agrees well with its corresponding data (open squares). This interference pattern is distinctly different from that obtained using a single-crystal configuration with the same overall nonlinear interaction length; it comprises two separate and disjoint fourth-order interference patterns. The theoretical results in the presence of 9-nm-bandwidth predetection filters, for the same two limits ($\phi_1 - \phi_2 = 0$ and $\phi_1 - \phi_2 = \pi/2$), are presented as the solid curves in Fig. 3, along with the associated experimental measurements (filled and open squares, respectively).

Conclusion.—We have measured the quantum-interference patterns for various separations between two parametric down-conversion nonlinear optical crystals, both with and without predetector spectral filters. In the unfiltered case, the quantum-interference patterns vary between two limiting forms. One is consistent with the coherent addition of contributions from the two crystals with $\phi_1 - \phi_2 = 0$; the other is consistent with coherent addition with $\phi_1 - \phi_2 = \pi/2$, which is also equivalent to incoherent addition. The presence of filters softens the interference patterns considerably; it also results in a

reduction of the entangled-photon-pair flux as is evident by comparing the ordinates in Figs. 2 and 3. The use of even narrower filters, with bandwidths from 1 to 3 nm such as those commonly used in quantum-interference experiments, results in a single-dip smooth interference pattern in both limits. The spectral preselection provided by the predetector filtering process therefore camouflages the unique mutual coherence properties of the twin-photon beams generated at the two crystals.

We conclude that nonclassical correlations and interference between probability amplitudes of entangled-photon pairs generated spontaneously from physically separate crystals yield controllable quantum-interference patterns. The ability to modify these patterns at will offers possibilities for quantum-state engineering. It is important to note that these novel effects are suppressed when spectral postselection is used, which is the usual practice.

This work was supported by the National Science Foundation.

-
- [1] S.E. Harris, M.K. Oshman, and R.L. Byer, *Phys. Rev. Lett.* **18**, 732 (1967); D. Magde and H. Mahr, *Phys. Rev. Lett.* **18**, 905 (1967); D.N. Klyshko, *Photons and Non-linear Optics* (Nauka, Moscow, 1980); J. Peřina, Z. Hradil, and B. Jurčo, *Quantum Optics and Fundamentals of Physics* (Kluwer, Boston, 1994); L. Mandel and E. Wolf, *Optical Coherence and Quantum Optics* (Cambridge, New York, 1995), Chap. 22.
- [2] J.S. Bell, *Physics* (Long Island City, N.Y.) **1**, 195 (1964); J.F. Clauser, M.A. Horne, A. Shimony, and R.A. Holt, *Phys. Rev. Lett.* **23**, 880 (1969); P.G. Kwiat, K. Mattle, H. Weinfurter, A. Zeilinger, A.V. Sergienko, and Y.H. Shih, *Phys. Rev. Lett.* **75**, 4337 (1995).
- [3] L. Hardy, *Phys. Rev. Lett.* **71**, 1665 (1993); A.G. White, D.F.V. James, P.H. Eberhard, and P.G. Kwiat, *Phys. Rev. Lett.* **83**, 3103 (1999).
- [4] D.M. Greenberger, M.A. Horne, and A. Zeilinger, in *Bell's Theorem, Quantum Theory, and Conceptions of the Universe*, edited by M. Kafatos (Kluwer, Dordrecht, 1989); D.M. Greenberger, M.A. Horne, A. Shimony, and A. Zeilinger, *Am. J. Phys.* **58**, 1131 (1990); D. Bouwmeester, J.-W. Pan, M. Daniell, H. Weinfurter, and A. Zeilinger, *Phys. Rev. Lett.* **82**, 1345 (1999).
- [5] D.N. Klyshko, *Sov. J. Quantum Electron.* **7**, 591 (1977); A. Migdall, R. Datla, A.V. Sergienko, J.S. Orszak, and Y.H. Shih, *Appl. Opt.* **37**, 3455 (1998).
- [6] B.E.A. Saleh, B.M. Jost, H.-B. Fei, and M.C. Teich, *Phys. Rev. Lett.* **80**, 3483 (1998); H.-B. Fei, B.M. Jost, S. Popescu, B.E.A. Saleh, and M.C. Teich, *Phys. Rev. Lett.* **78**, 1679 (1997).
- [7] B.M. Jost, A.V. Sergienko, A.F. Abouraddy, B.E.A. Saleh, and M.C. Teich, *Opt. Express* **3**, 81 (1998); B.E.A. Saleh, A.F. Abouraddy, A.V. Sergienko, and M.C. Teich, *Phys. Rev. A* **62**, 043816 (2000).
- [8] A.K. Ekert, *Phys. Rev. Lett.* **67**, 661 (1991); J.G. Rarity and P.R. Tapster, *Phys. Rev. A* **45**, 2052 (1992); J. Brendel, N. Gisin, W. Tittel, and H. Zbinden, *Phys. Rev. Lett.* **82**, 2594 (1999); A.V. Sergienko, M. Atatüre, Z. Walton, G. Jaeger, B.E.A. Saleh, and M.C. Teich, *Phys. Rev. A* **60**, R2622 (1999).
- [9] C.H. Bennett, G. Brassard, C. Crepeau, R. Jozsa, A. Peres, and W. Wootters, *Phys. Rev. Lett.* **70**, 1895 (1993); D. Boschi, S. Branca, F. De Martini, L. Hardy, and S. Popescu, *Phys. Rev. Lett.* **80**, 1121 (1998); D. Bouwmeester, J.-W. Pan, K. Mattle, M. Eibl, H. Weinfurter, and A. Zeilinger, *Nature (London)* **390**, 575 (1997).
- [10] G. Di Giuseppe, L. Haiberger, F. De Martini, and A.V. Sergienko, *Phys. Rev. A* **56**, R21 (1997); W.P. Grice, R. Erdmann, I.A. Walmsley, and D. Branning, *Phys. Rev. A* **57**, R2289 (1998); W.P. Grice and I.A. Walmsley, *Phys. Rev. A* **56**, 1627 (1997); T.E. Keller and M.H. Rubin, *Phys. Rev. A* **56**, 1534 (1997); J. Peřina, Jr., A.V. Sergienko, B.M. Jost, B.E.A. Saleh, and M.C. Teich, *Phys. Rev. A* **59**, 2359 (1999); D. Branning, W.P. Grice, R. Erdmann, and I.A. Walmsley, *Phys. Rev. Lett.* **83**, 955 (1999); T. Tsegaye, J. Söderholm, M. Atatüre, A. Trifonov, G. Björk, A.V. Sergienko, B.E.A. Saleh, and M.C. Teich, *Phys. Rev. Lett.* **85**, 5013 (2000).
- [11] M. Atatüre, A.V. Sergienko, B.M. Jost, B.E.A. Saleh, and M.C. Teich, *Phys. Rev. Lett.* **83**, 1323 (1999); M. Atatüre, A.V. Sergienko, B.E.A. Saleh, and M.C. Teich, *Phys. Rev. Lett.* **84**, 618 (2000).
- [12] X.Y. Zou, L.J. Wang, and L. Mandel, *Phys. Rev. Lett.* **67**, 318 (1991); D.N. Klyshko, *Sov. Phys. JETP* **77**, 222 (1993); L. Hardy, *Phys. Lett. A* **161**, 326 (1992); P.G. Kwiat, E. Waks, A.G. White, I. Appelbaum, and P.H. Eberhard, *Phys. Rev. A* **60**, R773 (1999).
- [13] M.M. Fejer, G.A. Magel, D.H. Jundt, and R.L. Byer, *IEEE J. Quantum Electron.* **11**, 2631 (1992); S. Tanzilli, H. De Riedmatten, W. Tittel, H. Zbinden, P. Baldi, M. De Micheli, D.B. Ostrowsky, and N. Gisin, *Electron. Lett.* **37**, 26 (2001).
- [14] M.H. Rubin, D.N. Klyshko, Y.H. Shih, and A.V. Sergienko, *Phys. Rev. A* **50**, 5122 (1994).